Human Herpesvirus 6 (HHV-6) Causes Severe Thymocyte Depletion in SCID-hu Thy/Liv Mice

By Alberto Gobbi,* Cheryl A. Stoddart,‡ Mauro S. Malnati,* Giuseppe Locatelli,* Fabio Santoro,* Nancy W. Abbey,§ Christopher Bare,‡ Valerie Linquist-Stepps,‡ Mary Beth Moreno,‡ Brian G. Herndier,§ Paolo Lusso,* and Joseph M. McCune‡

*From the *Unit of Human Virology, Department of Biological and Technological Research (DIBIT), San Raffaele Scientific Institute, Milan 20132, Italy; the ‡Gladstone Institute of Virology and Immunology, San Francisco, California 94110-9100; and the §Department of Pathology, University of California, San Francisco, California 94110*

Summary

Human herpesvirus 6 (HHV-6) is a potentially immunosuppressive agent that may act as a cofactor in the progression of AIDS. Here, we describe the first small animal model of HHV-6 infection. HHV-6 subgroup A, strain GS, efficiently infected the human thymic tissue implanted in SCID-hu Thy/Liv mice, leading to the destruction of the graft. Viral DNA was detected in Thy/Liv implants by quantitative polymerase chain reaction (PCR) as early as 4 d after inoculation and peaked at day 14. The productive nature of the infection was confirmed by electron microscopy and immunohistochemical staining. Atypical thymocytes with prominent nuclear inclusions were detected by histopathology. HHV-6 replication was associated with severe, progressive thymocyte depletion involving all major cellular subsets. However, intrathymic T progenitor cells (ITTPs) appeared to be more severely depleted than the other subpopulations, and a preferred tropism of HHV-6 for ITTPs was demonstrated by quantitative PCR on purified thymocyte subsets. These findings suggest that thymocyte depletion by HHV-6 may be due to infection and destruction of these immature T cell precursors. Similar results were obtained with strain PL-1, a primary isolate belonging to subgroup B. The severity of the lesions observed in this animal model underscores the possibility that HHV-6 may indeed be immunosuppressive in humans.

Key words: thymus gland • acquired immunodeficiency syndrome • T lymphocyte subsets • flow cytometry • polymerase chain reaction

Human herpesvirus 6 (HHV-6)[1] is a ubiquitous β-herpesvirus, first isolated from immunocompromised patients with various forms of lymphoproliferative disorders (1). All HHV-6 isolates can be classified into two subgroups, A and B. The B subgroup is predominant in the human population; it is associated with most of the cases of *exanthem subitum* in children, and its prevalence in healthy adults is almost universal. In contrast, no disease has been definitively linked to subgroup A, and its prevalence is still largely unknown. Because most of the A isolates have been derived from immunocompromised patients, this virus has been suggested to play a role in immunodeficiency, including AIDS (2).

HHV-6 has a primary tropism for mature $CD4^+$ T cells, both in vitro (3) and in vivo (4), and can also productively infect mature $CD8^+$ T cells, NK cells, γ/δ T cells (2), and thymocytes (3). HHV-6 exerts marked cytopathic effects in all of these cell types, suggesting that it may cause immunosuppression by infecting and destroying T cells or their precursors. Recently, HHV-6 has been implicated as a cause of severe progressive immunodeficiency in an HIV-1–seronegative infant (5). The patient had thymic atrophy and severe T lymphocytopenia associated with extensive HHV-6 infection of the thymus and lymph nodes.

Several lines of evidence suggest that HHV-6 may also function as a cofactor in AIDS, accelerating the progression towards the full-blown disease. In vitro studies have shown several positive interactions between HHV-6 and HIV-1,

Some of the results in this manuscript were presented at the Annual Meeting of the Institute of Human Virology, Baltimore, MD, August 1998.

[1]*Abbreviations used in this paper:* DAB, diaminobenzidine; DP, $CD3^-CD4^+CD8^+$ and $CD3^+CD4^+CD8^+$ double-positive; H&E, hematoxylin and eosin; HHV-6, human herpesvirus 6; ITTP, intrathymic T progenitor cell; SCID, severe combined immunodeficiency; SP4, mature $CD3^+CD4^+CD8^-$ single-positive 4; SP8, mature $CD3^+CD4^-CD8^+$ single-positive 8; $TCID_{50}$, 50% tissue culture infectious dose.

including the ability of HHV-6 to productively coinfect $CD4^+$ T lymphocytes with HIV-1, resulting in an enhanced cytopathic effect (6). HHV-6 can induce de novo expression of CD4 on cells that physiologically do not express it, such as mature $CD8^+$ T cells, NK cells, and γ/δ T cells, rendering them susceptible to HIV-1 infection (6). In vivo data indicate that HHV-6 infection is active and widespread in symptomatic HIV-infected patients (7–9), but definitive evidence of the immunosuppressive capability of HHV-6 and of its role in AIDS is still lacking.

One of the limitations hampering the elucidation of the pathogenic role of HHV-6 is that no reliable animal models of infection and pathogenesis by HHV-6 have been established to date, despite preliminary evidence indicating that the nonhuman primate *Macaca nemestrina* is susceptible to HHV-6 infection both in vitro (2) and in vivo (9a). SCID-hu Thy/Liv mice, obtained by coimplanting human fetal liver and thymus into immunodeficient SCID mice, are a well-established model for studying the pathogenesis of human viruses in vivo (10–18). After coimplantation under the murine kidney capsule, the human fetal tissues fuse, vascularize, and grow into a unique "Thy/Liv" organ that is morphologically and functionally equivalent to the human thymus (19, 20). This organ can be infected with human viruses by direct intrathymic injection. Thy/Liv implants are composed of five main thymocyte subpopulations that represent progressive stages of thymocyte maturation (21). The first stage is represented by a rare population with a triple-negative phenotype ($CD3^-CD4^-CD8^-$). Some of these cells differentiate into intrathymic T progenitor cells (ITTPs), which display a $CD3^-CD4^+CD8^-$ phenotype. This rapidly dividing population, which constitutes ~1–2% of the total thymocyte population, subsequently differentiates into $CD3^-CD4^+CD8^+$ and $CD3^+CD4^+CD8^+$ double-positive (DP) thymocytes. DP thymocytes are the most abundant subpopulation in Thy/Liv implants, accounting for ~80–85% of total thymocytes. Most of the DP thymocytes die within the thymus, but a fraction differentiates into mature $CD3^+CD4^+CD8^-$ single-positive 4 (SP4) and $CD3^+CD4^-CD8^+$ single-positive 8 (SP8) thymocytes. Specific tropisms of varicella zoster virus (16) and HIV-1 (11, 12, 14, 22) for different subpopulations of human thymocytes have been shown in SCID-hu Thy/Liv mice.

In this paper, we describe the effects of HHV-6 infection on the human thymus in SCID-hu Thy/Liv mice, focusing on the prototype HHV-6 subgroup A, strain GS (HHV-$6A_{GS}$). This strain was found to replicate efficiently in Thy/Liv implants and to induce severe depletion of thymocytes, supporting the hypothesis that it may act as an immunosuppressive agent in vivo. Similar results were obtained using HHV-$6B_{PL\text{-}1}$, a primary isolate belonging to subgroup B.

Materials and Methods

Inoculation of SCID-hu Thy/Liv Mice with HHV-6. SCID-hu Thy/Liv mice were obtained by coimplanting small pieces of human second trimester fetal liver and thymus under the kidney capsule of male homozygous CB-17 *scid/scid* (SCID) mice (20). Thy/Liv implants were infected 4–7 mo after implantation, as described (23). In brief, mice were anesthetized, the left kidney was surgically exposed, and the implant was inoculated with 25–50 μl of viral stock with a titer of 10^5 (strain GS) or 10^4 (strain PL-1) 50% tissue culture infectious doses ($TCID_{50}$) per 50 μl. UV-inactivated viral stock and culture medium were used for mock inoculations. The abdominal wall incision was sutured, and the skin was closed with staples. All procedures and practices were approved by the University of California, San Francisco Committee on Human Research or by the University of California, San Francisco Committee on Animal Research.

HHV-$6A_{GS}$, a primary subgroup A isolate, was obtained from cultures of purified human cord blood $CD4^+$ T cells infected with cell-free viral stock at a multiplicity of infection of 0.5. At day 6 after infection, the supernatants were collected, centrifuged at 2,500 *g*, and stored at −80°C. HHV-$6B_{PL\text{-}1}$, a primary subgroup B isolate, was obtained from in vitro–activated peripheral blood cells of a healthy adult blood donor and propagated for a single passage in activated cord blood $CD4^+$ T cells. No HHV-7 contamination was detected by nested PCR assay, and the stocks were also negative for *Mycoplasma*. Virus titration was performed by infecting triplicate cultures of phytohemagglutinin-activated human peripheral blood mononuclear cells with serial 10-fold dilutions of the viral stock.

Collection of Thy/Liv Implants from SCID-hu Mice. SCID-hu mice were killed by CO_2 inhalation, and implants were removed at different times after inoculation. Implants were processed for histopathology and electron microscopy as detailed below. For cytofluorimetric analysis, cell sorting, and quantitative PCR, single-cell suspensions were obtained by grinding the implants in a nylon bag. The cells were counted in a Coulter counter and divided into aliquots for the different assays.

Histology and Immunohistochemistry. Thy/Liv implants were fixed in 10% buffered formalin, embedded in paraffin, cut into 4-μm-thick sections, and stained with hematoxylin and eosin (H&E). For immunohistochemistry, unstained sections were pretreated with trypsin and pronase. The sections were then stained with a polyclonal antibody specific for CD3 (Dako) or an mAb specific for CD68 (Dako), using a standard peroxidase-labeled streptavidin-biotin (LSAB-peroxidase) method (LSAB2; Dako), followed by visualization with diaminobenzidine (DAB) and $CuSO_4$ enhancement (24). Before the second phase of staining, the samples were denatured in 2 N HCl for 10 min. The sections were then stained with 9A5D12, an mAb specific for the p41 early protein of HHV-6 (25). This antibody was revealed by a standard LSAB-alkaline phosphatase method (LSAB2; Dako) followed by visualization with Vector Red (Vector Laboratories). Negative controls included purified nonimmune mouse or rabbit serum (Dako), followed by LSAB-peroxidase staining. The sections were then denatured in HCl, and LSAB-alkaline phosphatase staining was carried out after incubation with either mouse serum (no stain) or 9A5D12 (red staining only).

Electron Microscopy. Small pieces of Thy/Liv implants were fixed in 2.5% glutaraldehyde, and samples were postfixed in osmium tetroxide, dehydrated in 2,2-dimethoxypropane, and embedded in Poly/Bed 812 resin (Polysciences, Inc.). Thin sections (600–900 Å) were cut with a diamond knife, mounted on copper grids, stained with uranyl acetate and lead citrate, and examined on a JEOL 100 SX electron microscope.

Cytofluorimetric Analysis and Cell Sorting. Single-cell suspensions were stained with an mAb cocktail containing CD4-FITC (Becton Dickinson), CD8-PE (Becton Dickinson), and CD3-tricolor

(CD3-TC) (Caltag). Cells were washed, resuspended in PBS containing 1% paraformaldehyde, and analyzed on a FACScan® (Becton Dickinson) for CD4, CD8, and CD3 expression after gating on a live-cell lymphoid population identified by forward- and side-scatter characteristics. For cell sorting, unfixed cells were stained as for FACS® analysis. A FACS Vantage™ (Becton Dickinson) was used to purify four populations of thymocytes: $CD3^+CD4^+CD8^-$ (SP4), $CD3^+CD4^-CD8^+$ (SP8), $CD3^+CD4^+CD8^+$ (DP), and $CD3^-CD4^+CD8^-$ (ITTP). Sorted cells were frozen as dry pellets and stored at −80°C for DNA extraction.

Quantitative PCR. DNA was extracted from frozen pellets by proteinase K digestion and purified by phenol-chloroform extraction by standard techniques. Viral load was quantitated with the TaqMan® fluorogenic detection system on an ABI Prism 7700 Sequence Detector® (Perkin-Elmer Applied Biosystems [26]). PCR was performed with primers 5′-CAAAGCCAAATTATCCAGAGCG-3′ and 5′-CGCTAGGTTGAGGATGATCGA-3′ and a probe located in the highly conserved open reading frame U67 of HHV-6 (27): 5′-CACCAGACGTCACACCCGAAGGAAT-3′. PCR amplification consisted of denaturation at 95°C for 15 min, followed by 40 cycles of denaturation at 95°C for 15 s and annealing/extension at 58°C for 60 s (Locatelli, G., F. Santoro, A. Gobbi, F. Veglia, P. Lusso, and M. Malnati, manuscript in preparation).

Statistical Analysis. Nonparametric statistical analyses were performed using the Mann-Whitney U test (StatView 5.0; Abacus Concepts).

Results

Replication of HHV-6A$_{GS}$ in Human Thy/Liv Implants. 58 SCID-hu Thy/Liv mice from 6 different cohorts, each made with tissues from a single fetal donor, were inoculated with HHV-6 by direct intrathymic injection of 10^5 $TCID_{50}$ of strain GS or mock infected with UV-inactivated viral stock or with cell culture medium. Mice were killed 4, 7, 11, 14, and 27 d after inoculation, and the implants were removed. Viral replication was monitored by quantitative PCR on total thymocyte suspensions with the TaqMan® real time detection system. HHV-6 DNA was detected as early as 4 d after inoculation in each of the three implants examined (Fig. 1). The viral load peaked on day 14 with a mean value of ~6,000 copies/10^3 cells. In the implants harvested 27 d after inoculation, a drastic reduction in the number of genomic copies, with a mean of ~400 copies/10^3 cells, was observed (Fig. 1). No HHV-6 DNA was detected in the mock-infected control implants. The productive nature of HHV-6A$_{GS}$ infection in Thy/Liv implants was demonstrated by transmission electron microscopy showing viral particles at different stages of maturation (Fig. 2). In particular, naked viral nucleocapsids were observed in the nucleus, tegument-coated particles in the cytoplasm (not shown),

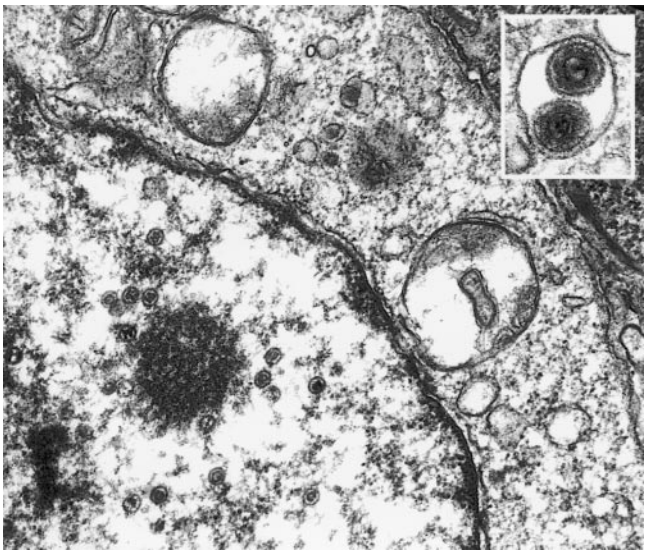

Figure 2. Transmission electron microscopy of a Thy/Liv implant harvested 11 d after inoculation with HHV-6A$_{GS}$. Naked viral nucleocapsids are visible in the nucleus, and two mature virions are visible in a cytoplasmic vacuole (insert). Original magnifications: ×10,000; inset, ×40,000.

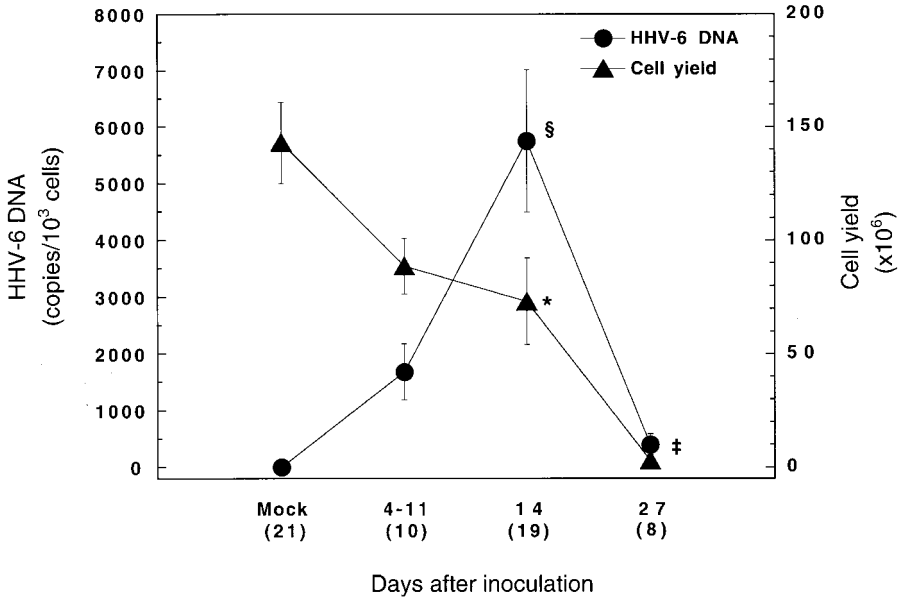

Figure 1. Replication of HHV-6A$_{GS}$ in Thy/Liv implants. Implants were harvested 4, 7, 11, 14, and 27 d after direct intrathymic injection with HHV-6A$_{GS}$ or mock injection of UV-inactivated viral stock (n = 9) or culture medium (n = 12) (Mock). Data obtained at day 4, 7, and 11 were pooled. The amount of HHV-6 DNA and cell yield per implant are shown as means ± SEM. The numbers in parentheses indicate the number of mice analyzed at each of the indicated time points. Results include three independent experiments with six different cohorts of SCID-hu Thy/Liv mice. *$P <$ 0.01, ‡$P < 0.001$ vs. mock; §$P < 0.05$ vs. days 4–11, and $P < 0.001$ vs. day 27.

and mature, enveloped virions in cytoplasmic vacuoles. This pattern is consistent with the documented ultrastructural development of HHV-6 in cells infected in vitro (28).

Thymocyte Depletion and Histopathological Changes in Thy/Liv Implants Infected with HHV-6A$_{GS}$. HHV-6A$_{GS}$ infection of Thy/Liv implants was associated with a marked, progressive depletion of thymocytes (Fig. 1). The number of thymocytes harvested from the HHV-6A$_{GS}$–infected implants was significantly reduced at day 14 ($P < 0.01$) compared with mock-infected implants and was reduced by >98% by day 27 ($P < 0.001$). A representative HHV-6A$_{GS}$–infected Thy/Liv implant is shown in Fig. 3 A. Compared with the mock-infected implant shown in Fig. 3 B, the HHV-6A$_{GS}$–infected thymus had a marked expansion of the medullary zone, apparent destruction or compression of the cortical zone, and destruction of the corticomedullary junction (Fig. 3 A). The medullary expansion appeared to be driven by endothelial proliferation or by vascular ectasia and fibrocyte proliferation. The endothelial cells lining medullary vessels appeared to be activated, in a fashion resembling vascular endothelium in the setting of inflammation. The expanded medullary zone contained atypical cells with prominent nuclear inclusions (Cowdry type A; Fig. 3 C). Immunohistochemical staining with an mAb specific for the p41 early protein of HHV-6 demonstrated that most of these atypical cells were infected (Fig. 3 D). Double-staining analysis showed that virtually all the infected cells were CD3$^+$, albeit with varying degrees of intensity (Fig. 3 E). By contrast, double-label staining with CD68 did not indicate a tropism of HHV-6A$_{GS}$ for macrophages in this model (Fig. 3 F).

Cytofluorimetric Analysis of Thymocyte Subpopulations from Thy/Liv Implants Infected with HHV-6A$_{GS}$. To evaluate the effects of viral replication on different thymocyte subpopulations, we performed quantitative flow cytometry on total thymocyte suspensions obtained from six different cohorts of SCID-hu Thy/Liv mice in three independent experiments. HHV-6A$_{GS}$–infected implants were harvested 4, 7, 11, 14, and 27 d after inoculation and examined for expression of CD3, CD4, and CD8. 4 and 7 d after inoculation,

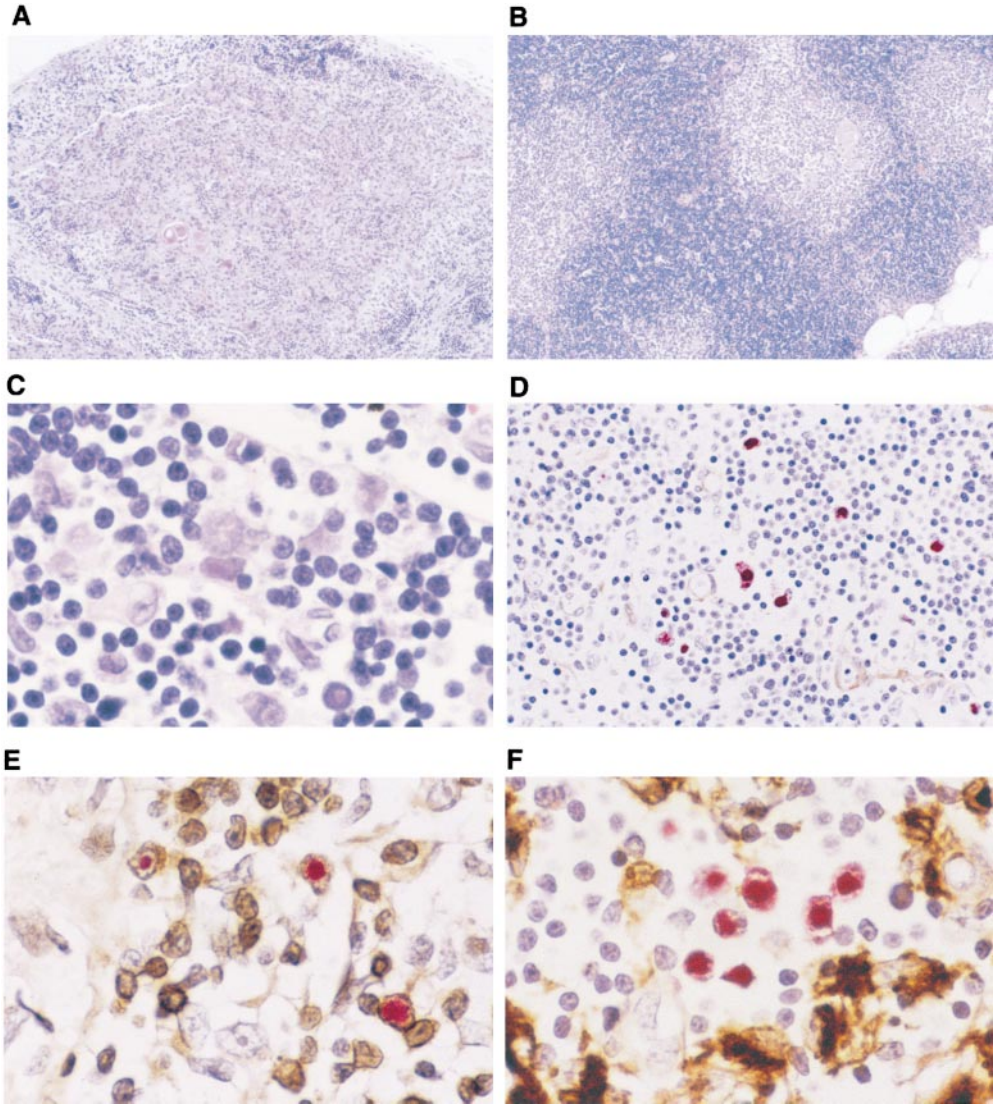

Figure 3. Histopathology of HHV-6A$_{GS}$–infected Thy/Liv implants. (A) Severe thymocyte depletion associated with proliferation of granulation tissue in an implant harvested 14 d after inoculation with HHV-6A$_{GS}$ (H&E; original magnification: ×40). (B) Typical appearance of a mock-infected Thy/Liv implant (H&E; original magnification: ×40). (C) Cytopathic effects induced by HHV-6A$_{GS}$. Atypical giant cells with prominent nuclear viral inclusions (Cowdry type A) (H&E; original magnification: ×1,000). (D) Immunohistochemical staining with 9A5D12, an mAb specific for the p41 early protein of HHV-6. Infected cells are scattered throughout the implant and include several large atypical cells (original magnification: ×100). (E) Double staining with CD3 (DAB) and 9A5D12 (Vector Red). All the cells that are positive for HHV-6 also coexpress CD3 (original magnification: ×1,000). (F) Double staining with an mAb to the macrophage marker CD68 (DAB) and to the p41 early protein of HHV-6 (9A5D12, Vector Red) (original magnification: ×1,000).

Table I. *Effects of HHV-6A$_{GS}$ Replication on Thymocyte Subpopulations*

Days after inoculation	No. of mice	Live thymocytes*	DP‡	SP4‡	SP8‡	ITTP‡
		%	%	%	%	%
Mock	21	70 ± 1.5	86 ± 0.6	8.7 ± 0.4	4.4 ± 0.3	1.4 ± 0.1
4	3	76 ± 0.8	87 ± 1.5	8.2 ± 1.2	4.6 ± 0.4	0.8 ± 0.1
7	3	64 ± 6.6	87 ± 2.2	6.9 ± 1.3	5.2 ± 0.9	0.9 ± 0.4
11	4	50 ± 8.6	85 ± 0.9	9.5 ± 1.0	4.6 ± 0.3	0.3 ± 0.1§
14	19	53 ± 4.8§	79 ± 1.5‖	12 ± 1.1§	6.5 ± 0.4‖	1.0 ± 0.2§
27	8	6.7 ± 3.9‖	ND	ND	ND	ND

Thy/Liv implants were harvested 4, 7, 11, 14, and 27 d after direct intrathymic injection of HHV-6A$_{GS}$ or mock injection of UV-inactivated viral stock ($n = 9$) or culture medium ($n = 12$) (Mock) and assessed for distribution of thymocyte subpopulations by flow cytometry.
*The percentage of live thymocytes was determined by forward- and side-scatter characteristics.
‡Thymocyte subsets were quantified as a percentage of total live thymocytes. Data are expressed as mean ± SEM of three independent experiments using six different cohorts of SCID-hu Thy/Liv mice.
§$P < 0.01$ vs. mock-infected implants.
‖$P < 0.001$ vs. mock-infected implants.

the percentages of the different thymocyte subsets were unchanged compared with mock-infected implants (Table I). The earliest detectable phenotypic change was a reduced percentage of ITTPs at day 11 ($P < 0.05$), a time at which the percentages of the other thymocyte subpopulations were not yet significantly changed (Table I). By day 14, a reduction in the percentage of live thymocytes, identified by forward- and side-scatter profiles, was observed (Table I). At this time point, ITTPs remained significantly depleted ($P < 0.01$), and there was also a reduction in the percentage of DP thymocytes ($P < 0.001$) and an increase in the percentage of SP4 ($P < 0.05$) and SP8 ($P < 0.01$) thymocytes (Table I). By day 27, most of the thymocytes were dead or dying, and it was no longer possible to analyze the different subpopulations (Table I).

Cellular Tropism of HHV-6A$_{GS}$ in Thy/Liv Implants. To study the cellular tropism of HHV-6A$_{GS}$ in Thy/Liv implants, the distribution of viral DNA was quantitated in the different subpopulations of thymocytes as a function of time after inoculation. Total thymocytes were harvested at 4, 7, 11, and 14 d after inoculation and sorted into DP, SP4, SP8, and ITTP subpopulations. The viral load in each subpopulation was measured by quantitative PCR (Table II). At day 4 after inoculation, viral DNA was detectable in ITTPs but was less abundant or undetectable in the other subpopulations. By day 7, HHV-6 DNA was detectable in all the thymocyte subsets, but was significantly more abundant in ITTPs ($P < 0.05$) and remained so at 11 and 14 d after inoculation. No HHV-6 DNA was detected in any of the thymocyte subpopulations from Thy/Liv implants infected with UV-inactivated viral stock (data not shown).

Replication of HHV-6B$_{PL-1}$ in Human Thy/Liv Implants. To study the effects of HHV-6 subgroup B on Thy/Liv implants, six SCID-hu Thy/Liv mice were inoculated with 10^4 TCID$_{50}$ of strain PL-1 (a primary isolate passaged in vitro only twice), or mock infected with cell culture me-

Table II. *Cellular Tropism of HHV-6A$_{GS}$ in Thy/Liv Implants*

Days after inoculation	No. of mice	HHV-6 DNA (copies/10^3 cells)*			
		DP	SP4	SP8	ITTP
4	3	Undetectable‡	Undetectable‡	20 ± 20	123 ± 91
7	3	23 ± 23	497 ± 304	140 ± 72	1,500 ± 863§
11	3	280 ± 181	Undetectable‡	30 ± 30	6,840 ± 4,645‖
14	7	32 ± 17	33 ± 18	45 ± 22	599 ± 323‖

Thy/Liv implants were harvested 4, 7, 11, and 14 d after direct intrathymic injection of HHV-6A$_{GS}$. DP, SP4, SP8 thymocytes, and ITTPs were then sorted, and HHV-6 DNA load was assessed by quantitative PCR.
*Mean viral copies/10^3 cells ± SEM. Results are shown from two independent experiments in three different cohorts of SCID-hu Thy/Liv mice.
‡Less than 10 copies/10^3 cells.
§$P < 0.05$ vs. DP and SP8 thymocytes.
‖$P < 0.05$ vs. DP, SP4, and SP8 thymocytes.

dium. Mice were killed 10 d after inoculation, and the implants were removed. Quantitative PCR analysis revealed efficient replication of HHV-$6B_{PL-1}$ (mean viral load of ~2,200 copies/10^3 cells) similar to that found in HHV-$6A_{GS}$–infected implants (Table III). The effects of HHV-$6B_{PL-1}$ replication on thymocyte subpopulations were assessed by flow cytometry. As observed for strain GS at a similar time point (day 11; Table I), the main effect of HHV-$6B_{PL-1}$ on thymocyte subpopulations was a reduction in the percentage of ITTPs (Table III). At this relatively early time point, the percentage of live thymocytes was also decreased (Table III).

Discussion

This study provides the first evidence that HHV-6 can replicate in the human thymus in vivo, leading to a progressive destruction of the organ. The severity of the lesions caused by HHV-6 in Thy/Liv implants supports the hypothesis that this virus may be immunosuppressive, as previously suggested by its tropism for $CD4^+$ T cells and by the severe cytopathic effects it exerts on infected cells in vitro. Interestingly, the histological lesions we observed in HHV-6–infected Thy/Liv implants are similar to those recently described in the thymus of an HIV-1–negative infant with immunosuppression associated with widespread HHV-6 infection (5), suggesting that SCID-hu Thy/Liv mice may reproduce the pathological mechanisms of HHV-6 infection in humans. However, despite the high prevalence of HHV-6 infection in the human population, only rare cases of putative HHV-6–related immunosuppression have been reported to date. It remains to be determined whether thymic infection by HHV-6 is an uncommon occurrence or, alternatively, whether its pathological consequences in vivo may be attenuated by host immune responses.

The experiments reported here were focused mainly on HHV-$6A_{GS}$, but limited studies with a subgroup B virus (PL-1) indicate that viruses of both subgroups can replicate in the Thy/Liv organ and induce cytopathicity. Clinical and epidemiological studies have shown an association of both subgroup A and B viruses with immunodeficiency (2), although subgroup B viruses have also been frequently isolated from the general population of nonimmunocompromised subjects. Coinfection by A and B strains was also documented in the infant with HHV-6–associated immunosuppression mentioned above (5). Further work will be required, both in humans and in SCID-hu Thy/Liv mice, to determine whether there are any intrinsic differences between the two HHV-6 subgroups in their propensity to induce immunosuppression in vivo.

The immunohistochemical detection of the CD3 antigen on the majority of the infected cells suggests that mature thymocytes can be infected by HHV-6 in vivo. However, the early and persistent depletion of ITTPs indicates that HHV-6 has a particular tropism for these immature cells. Indeed, quantitative PCR on sorted thymocyte subpopulations showed a markedly higher HHV-6 DNA load in ITTPs than in the other subpopulations. ITTPs are a relatively rare but rapidly dividing subpopulation that represents an early step of thymocyte maturation and gives rise to DP thymocytes and their mature SP progeny (21). Destruction of ITTPs may result in the generalized suppression of thymopoiesis and ultimately in the depletion of the thymus.

The thymus is the primary site of T lymphocyte development in utero and in early life. Although its activity diminishes progressively with age, this organ may still be functional in adults and, during conditions of severe T cell depletion (including HIV-1 infection), it may play an important role in maintaining and reconstituting the peripheral immune system (29–32). Accordingly, abundant thymic tissue has been detected by chest computed tomography in HIV-1–seropositive adults, suggesting that thymic function may be enhanced, by a compensatory mechanism, in some HIV-1–infected patients (32). However, persistent thymic function in an adult could be quickly abolished by thymic infection with HIV or other T cell–tropic viruses such as HHV-6.

Because of its tropism for $CD4^+$ T lymphocytes and its positive interactions in vitro with HIV-1, HHV-6 has been suggested as a possible cofactor in AIDS (6). This hypothesis is supported by clinical evidence of active and widespread HHV-6 infection in symptomatic AIDS patients (7–9).

Table III. *Replication of HHV-$6B_{PL-1}$ in Thy/Liv Implants and Effects on Thymocyte Subpopulations*

Virus	No. of mice	HHV-6 DNA*	Live thymocytes‡	DP§	SP4§	SP8§	ITTP§
			%	%	%	%	%
Mock	2	Undetectable	73 ± 9.1	82 ± 0.4	10.4 ± 0.1	6.4 ± 0.1	1.2 ± 0.1
HHV-$6B_{PL-1}$	4	2,169 ± 552	62 ± 2.5	82 ± 0.4	8.8 ± 0.3	8.1 ± 0.3	0.3 ± 0.02

Thy/Liv implants were harvested 10 d after direct intrathymic injection of HHV-$6B_{PL-1}$ or mock injection of culture medium. Viral replication was assessed by quantitative PCR on total thymocyte suspensions, and the distribution of thymocyte subpopulations was studied by flow cytometry.
*Mean viral copies/10^3 cells ± SEM.
‡The percentage of live thymocytes was determined by forward- and side-scatter characteristics.
§Thymocyte subsets were quantified as a percentage of total live thymocytes. Data are expressed as mean ± SEM.

HHV-6 infects human thymocytes in vitro (3) and has been detected in the thymus in vivo (5, 33). Thus, HHV-6 infection of the thymus may play a role in the immunodeficiency associated with HIV-1 infection. However, it is technically difficult to study the thymus in humans, and no reports are currently available on the presence of thymic HHV-6 infection in patients with HIV disease. The SCID-hu Thy/Liv mouse model, carrying a human graft that is morphologically and functionally equivalent to the human thymus, provides a unique system to study the pathogenesis of HHV-6 and HIV-1 infections in vivo (10–14). Interestingly, some chemokine receptor CXCR4-using strains of HIV-1, like NL4-3, suppress thymopoiesis in SCID-hu Thy/Liv mice by direct infection and destruction of ITTPs (11). The tropism of HHV-6 and HIV-1 for the same thymocyte subset raises the possibility of synergistic interactions in the thymic environment. Future studies of coinfection with HHV-6 and HIV-1 in SCID-hu Thy/Liv mice may provide important insights into the role of HHV-6 in HIV-1 disease.

We thank Morgan Jenkins for critical review of this manuscript, Stephen Ordway and Gary Howard for editing the manuscript, and Lisa Gibson and Eric Wieder for assistance with cell sorting.

This work was supported by European Union Biomed 2 grant PL951301 and Istituto Superiore di Sanità-Rome grant 40A059 (to P. Lusso), and by National Institute of Allergy and Infectious Diseases grants AI40312, AI65309 (to J.M. McCune), and CA73534 (to B.G. Herndier). J.M. McCune is an Elizabeth Glaser Scientist supported by the Elizabeth Glaser Pediatric AIDS Foundation.

Address correspondence to Joseph M. McCune, Gladstone Institute of Virology and Immunology, P.O. Box 419100, San Francisco, CA 94110-9100. Phone: 415-695-3828; Fax: 415-826-8449; E-mail: mmccune@gladstone.ucsf.edu

Received for publication 5 March 1999 and in revised form 20 April 1999.

References

1. Salahuddin, S.Z., D.V. Ablashi, P.D. Markham, S.F. Josephs, S. Sturzenegger, M. Kaplan, G. Halligan, P. Biberfeld, F. Wong-Staal, B. Kramarsky, and R.C. Gallo. 1986. Isolation of a new virus, HBLV, in patients with lymphoproliferative disorders. *Science*. 234:596–601.
2. Lusso, P. 1996. Human herpesvirus 6 (HHV-6). *Antiviral Res*. 31:1–21.
3. Lusso, P., P.D. Markham, E. Tschachler, F. di Marzo Veronese, S.Z. Salahuddin, D.V. Ablashi, S. Pahwa, K. Krohn, and R.C. Gallo. 1988. In vitro cellular tropism of human B-lymphotropic virus (human herpesvirus-6). *J. Exp. Med*. 167:1659–1670.
4. Takahashi, K., S. Sonoda, K. Higashi, T. Kondo, H. Takahashi, M. Takahashi, and K. Yamanishi. 1989. Predominant CD4 T-lymphocyte tropism of human herpesvirus 6-related virus. *J. Virol*. 63:3161–3163.
5. Knox, K.K., D. Pietryga, D.J. Harrington, R. Franciosi, and D.R. Carrigan. 1995. Progressive immunodeficiency and fatal pneumonitis associated with human herpesvirus 6 infection in an infant. *Clin. Infect. Dis*. 20:406–413.
6. Lusso, P., and R.C. Gallo. 1995. Human herpesvirus 6 in AIDS. *Immunol. Today*. 16:67–71.
7. Corbellino, M., P. Lusso, R.C. Gallo, C. Parravicini, M. Galli, and M. Moroni. 1993. Disseminated human herpesvirus 6 infection in AIDS. *Lancet*. 342:1242.
8. Knox, K.K., and D.R. Carrigan. 1994. Disseminated active HHV-6 infections in patients with AIDS. *Lancet*. 343:577–578.
9. Secchiero, P., D.R. Carrigan, Y. Asano, L. Benedetti, R.W. Crowley, A.L. Komaroff, R.C. Gallo, and P. Lusso. 1995. Detection of human herpesvirus 6 in plasma of children with primary infection and immunosuppressed patients by polymerase chain reaction. *J. Infect. Dis*. 171:273–280.

9a. Lusso, P., R.W. Crowley, P. Secchiero, J.L. Southers, P.D. Markham, G. Franchini, and R.C. Gallo. 1995. Experimental coinfection in vivo by SIVSM and HHV-6GS in *Macaca nemestrina*. *AIDS Res. Hum. Retrovir*. 11:S100. (Abstr.)

10. Namikawa, R., H. Kaneshima, M. Lieberman, I.L. Weissman, and J.M. McCune. 1988. Infection of the SCID-hu mouse by HIV-1. *Science*. 242:1684–1686.
11. Su, L., H. Kaneshima, M. Bonyhadi, S. Salimi, D. Kraft, L. Rabin, and J.M. McCune. 1995. HIV-1-induced thymocyte depletion is associated with indirect cytopathogenicity and infection of progenitor cells in vivo. *Immunity*. 2:25–36.
12. Stanley, S.K., J.M. McCune, H. Kaneshima, J.S. Justement, M. Sullivan, E. Boone, M. Baseler, J. Adelsberger, M. Bonyhadi, J. Orenstein, et al. 1993. Human immunodeficiency virus infection of the human thymus and disruption of the thymic microenvironment in the SCID-hu mouse. *J. Exp. Med*. 178:1151–1163.
13. Bonyhadi, M.L., L. Rabin, S. Salimi, D.A. Brown, J. Kosek, J.M. McCune, and H. Kaneshima. 1993. HIV induces thymus depletion in vivo. *Nature*. 363:728–732.
14. Aldrovandi, G.M., G. Feuer, L. Gao, B. Jamieson, M. Kristeva, I.S. Chen, and J.A. Zack. 1993. The SCID-hu mouse as a model for HIV-1 infection. *Nature*. 363:732–736.
15. Mocarski, E.S., M. Bonyhadi, S. Salimi, J.M. McCune, and H. Kaneshima. 1993. Human cytomegalovirus in a SCID-hu mouse: thymic epithelial cells are prominent targets of viral replication. *Proc. Natl. Acad. Sci. USA*. 90:104–108.
16. Moffat, J.F., M.D. Stein, H. Kaneshima, and A.M. Arvin. 1995. Tropism of varicella-zoster virus for human CD4+ and CD8+ T lymphocytes and epidermal cells in SCID-hu mice. *J. Virol*. 69:5236–5242.
17. Auwaerter, P.G., H. Kaneshima, J.M. McCune, G. Wiegand, and D.E. Griffin. 1996. Measles virus infection of thymic epithelium in the SCID-hu mouse leads to thymocyte apop-

tosis. *J. Virol*. 70:3734–3740.
18. Feuer, G., J.K. Fraser, J.A. Zack, F. Lee, R. Feuer, and I.S. Chen. 1996. Human T-cell leukemia virus infection of human hematopoietic progenitor cells: maintenance of virus infection during differentiation in vitro and in vivo. *J. Virol*. 70: 4038–4044.
19. Krowka, J.F., S. Sarin, R. Namikawa, J.M. McCune, and H. Kaneshima. 1991. Human T cells in the SCID-hu mouse are phenotypically normal and functionally competent. *J. Immunol*. 146:3751–3756.
20. Namikawa, R., K.N. Weilbaecher, H. Kaneshima, E.J. Yee, and J.M. McCune. 1990. Long-term human hematopoiesis in the SCID-hu mouse. *J. Exp. Med*. 172:1055–1063.
21. Kraft, D.L., I.L. Weissman, and E.K. Waller. 1993. Differentiation of $CD3^-4^-8^-$ human fetal thymocytes in vivo: characterization of a $CD3^-4^+8^-$ intermediate. *J. Exp. Med*. 178: 265–277.
22. Jenkins, M., M.B. Hanley, M.B. Moreno, E. Wieder, and J.M. McCune. 1998. Human immunodeficiency virus-1 infection interrupts thymopoiesis and multilineage hematopoiesis in vivo. *Blood*. 91:2672–2678.
23. Rabin, L., M. Hincenbergs, M.B. Moreno, S. Warren, V. Linquist, R. Datema, B. Charpiot, J. Seifert, H. Kaneshima, and J.M. McCune. 1996. Use of standardized SCID-hu Thy/Liv mouse model for preclinical efficacy testing of anti-human immunodeficiency virus type 1 compounds. *Antimicrob. Agents Chemother*. 40:755–762.
24. Orenstein, J.M., S. Alkan, A. Blauvelt, K.T. Jeang, M.D. Weinstein, D. Ganem, and B. Herndier. 1997. Visualization of human herpesvirus type 8 in Kaposi's sarcoma by light and transmission electron microscopy. *AIDS*. 11:F35–F45.
25. Balachandran, N., R.E. Amelse, W.W. Zhou, and C.K. Chang. 1989. Identification of proteins specific for human herpesvirus 6-infected human T cells. *J. Virol*. 63:2835–2840.
26. Heid, C.A., J. Stevens, K.J. Livak, and P.M. Williams. 1996. Real time quantitative PCR. *Genome Res*. 6:986–994.
27. Gompels, U.A., J. Nicholas, G. Lawrence, M. Jones, B.J. Thomson, M.E. Martin, S. Efstathiou, M. Craxton, and H.A. Macaulay. 1995. The DNA sequence of human herpesvirus-6: structure, coding content, and genome evolution. *Virology*. 209:29–51.
28. Biberfeld, P., B. Kramarsky, S.Z. Salahuddin, and R.C. Gallo. 1987. Ultrastructural characterization of a new human B lymphotropic DNA virus (human herpesvirus 6) isolated from patients with lymphoproliferative disease. *J. Natl. Cancer Inst*. 79:933–941.
29. McCune, J.M. 1997. Thymic function in HIV-1 disease. *Semin. Immunol*. 9:397–404.
30. Gaulton, G.N., J.V. Scobie, and M. Rosenzweig. 1997. HIV-1 and the thymus. *AIDS*. 11:403–414.
31. Douek, D.C., R.D. McFarland, P.H. Keiser, E.A. Gage, J.M. Massey, B.F. Haynes, M.A. Polis, A.T. Haase, M.B. Feinberg, J.L. Sullivan, et al. 1998. Changes in thymic function with age and during the treatment of HIV infection. *Nature*. 396:690–695.
32. McCune, J.M., R. Loftus, D.K. Schmidt, P. Carroll, D. Webster, L.B. Swor-Yim, I.R. Francis, B.H. Gross, and R.M. Grant. 1998. High prevalence of thymic tissue in adults with human immunodeficiency virus-1 infection. *J. Clin. Invest*. 101:2301–2308.
33. Aubin, J.T., L. Poirel, H. Agut, J.M. Huraux, C. Bignozzi, Y. Brossard, N. Mulliez, J. Roume, F. Lecuru, and R. Taurelle. 1992. Intrauterine transmission of human herpesvirus 6. *Lancet*. 340:482–483.